Journal of Alloys and Compounds 562 (2013) 219–223

Contents lists available at SciVerse ScienceDirect

Journal of Alloys and Compounds

journal homepage: www.elsevier.com/locate/jalcom

Thermal stability of charged $LiNi_{0.5}Co_{0.2}Mn_{0.3}O_2$ cathode for Li-ion batteries investigated by synchrotron based in situ X-ray diffraction

Yong-Hun Cho [a], Donghyuk Jang [b], Jeongbae Yoon [b], Hyunchul Kim [b], Tae Kyu Ahn [b], Kyung-Wan Nam [c], Yung-Eun Sung [d], Woo-Seong Kim [e], Yun-Sung Lee [f], Xiao-Qing Yang [c], Won-Sub Yoon [b,*]

[a] School of Advanced Materials Engineering, Kookmin University, 861-1 Jeongneung-dong, Seongbuk-gu, Seoul 136-702, Republic of Korea
[b] Department of Energy Science, Sungkyunkwan University, 300 Suwon-si, Gyeonggi-do 440-746, Republic of Korea
[c] Chemistry Department, Brookhaven National Laboratory, Upton, NY 11973, USA
[d] World Class University (WCU) Program of Chemical Convergence for Energy & Environment (C2E2), School of Chemical and Biological Engineering, College of Engineering, Seoul National University (SNU), Seoul 151-744, Republic of Korea
[e] Daejung EM Co. Ltd., Incheon 405-820, Republic of Korea
[f] Faculty of Applied Chemical Engineering, Chonnam National University, Gwang-ju 500-757, Republic of Korea

ARTICLE INFO

Article history:
Received 17 December 2012
Received in revised form 13 February 2013
Accepted 13 February 2013
Available online 26 February 2013

Keywords:
Lithium battery
Thermal stability
High nickel layered compounds
In situ X-ray diffraction
Phase transition

ABSTRACT

Structural changes for $LiNi_{0.5}Co_{0.2}Mn_{0.3}O_2$ cathode material of lithium-ion battery with and without electrolyte during heating from 25 to 600 °C are investigated using synchrotron based in situ X-ray diffraction. $LiNi_{0.5}Co_{0.2}Mn_{0.3}O_2$ without electrolyte first converts from a layered structure to disordered LiM_2O_4-type spinel and M_3O_4-type spinel phase as the temperature increases, then two different types of disordered spinel phases are co-existed up to 600 °C and no further decomposition to MO-type rock salt phase is presented at all. The electrolyte accelerates the thermal decomposition of the charged cathode materials. The presence of the electrolyte alters the paths of the structural changes and lowers the onset temperatures of the thermal decomposition reactions. In the case of $LiNi_{0.5}Co_{0.2}Mn_{0.3}O_2$ with electrolyte, more dramatic structural changes are observed compared with $LiNi_{0.5}Co_{0.2}Mn_{0.3}O_2$ without electrolyte and MO-type rock salt phase and metallic phase are presented at the end of the heating.

1. Introduction

Li-ion batteries (LIBs) are currently of interest because of their highest energy density among all rechargeable batteries for an application to transportation such as electric vehicle, hybrid electric vehicle and plug-in hybrid electric vehicle. The application of LIB to transportation needs large scale up for requiring power. However, arising safety problem such as thermal instability will be inevitable by scale up of battery cell because of the occurrence of exothermic reactions in charged batteries at elevated temperature. The catastrophic failure of the battery can be regarded as a result of the thermal runaway which has been attributed to the reactions between the charged electrodes and electrolyte [1–3]. Recently, $LiNi_{1-y-z}Mn_yCo_zO_2$ cathode materials have attracted a lot of interest due to its advantages such as low cost, high specific capacity, and good thermal stability [4–9]. Above all things, the thermal stability of the cathode material is very important. $LiNi_{1-y-z}Mn_yCo_zO_2$ is isostructural to α-$NaFeO_2$. Most of transition metal ions exist in 3b site. Each transition metal ion plays an important role on the electrode performance. For example, Ni ions give high capacity. Co ions improve layered characteristics. Mn ions stabilize the layered structure [10–15]. Therefore, optimization of the ratio of each ion is crucial to the electrode performance. $LiNi_{0.5}Co_{0.2}Mn_{0.3}O_2$ is one of the optimized compositions in $LiNi_{1-y-z}Mn_yCo_zO_2$ cathode materials series, which is now commercialized in some of the major battery companies [16–20]. When more Ni ions are introduced in the layered structure, more capacity is realized in the expense of the stability of the electrode material. In order to understand thermal stability of the charged $LiNi_{0.5}Co_{0.2}Mn_{0.3}O_2$ electrodes in Li-ion cells, we have thoroughly investigated the structural changes of the charged $LiNi_{0.5}Co_{0.2}Mn_{0.3}O_2$ cathode materials with and without electrolyte during heating up to 600 °C by using synchrotron based in situ X-ray diffraction technique. This thermal structure study gives a better understanding of the thermal stability of high nickel-containing $LiNi_{1-y-z}Mn_yCo_zO_2$ layered cathode materials.

2. Experimental

Firstly, $(Ni_{0.5}Co_{0.2}Mn_{0.3})\cdot(OH)_2$ was synthesized from $NiSO_4\cdot 6H_2O$ (Jinlin Jien, China), $MnSO_4\cdot H_2O$ (Chuo Denki, Japan), and $CoSO_4\cdot 7H_2O$ (Jinlin Jien, China) using a conventional co-precipitation method [21,22]. A stoichiometric amount of each material (Ni:Co:Mn = 0.5:0.2:0.3) was dissolved in purified, ion-exchanged water to prepare an aqueous metal solution. The reaction was performed for 48 h to

* Corresponding author. Tel.: +82 31 299 6276; fax: +82 31 299 4279.
E-mail address: wsyoon@skku.edu (W.-S. Yoon).

0925-8388/$ - see front matter © 2013 Elsevier B.V. All rights reserved.
http://dx.doi.org/10.1016/j.jallcom.2013.02.060

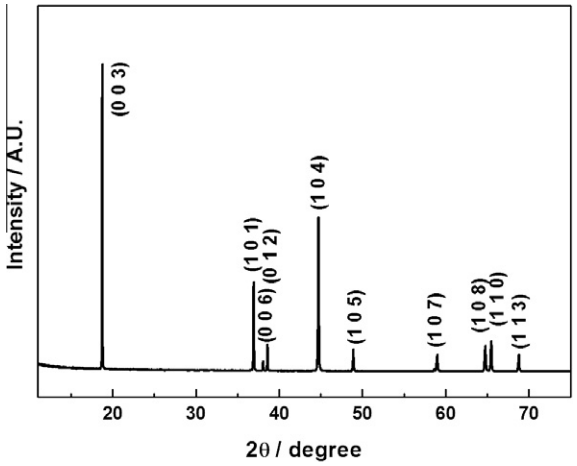

Fig. 1. High resolution X-ray diffraction pattern of $LiNi_{0.5}Co_{0.2}Mn_{0.3}O_2$ powders.

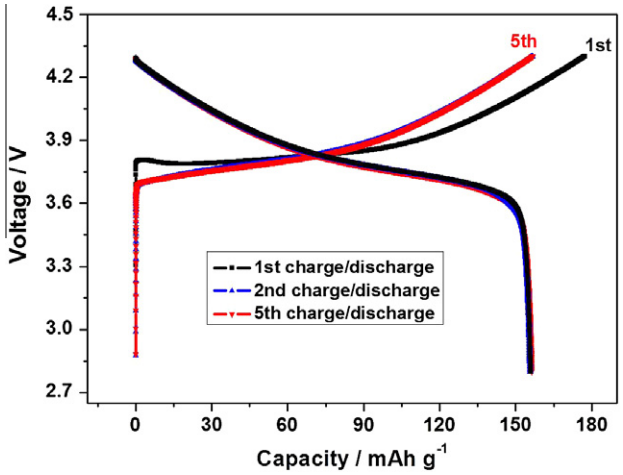

Fig. 2. Charge/discharge curves of $Li/LiNi_{0.5}Co_{0.2}Mn_{0.3}O_2$ cell at rate of C/10 between 2.8 and 4.3 V.

obtain a slurry containing a composite metal hydroxide with uniform size. The slurry was washed and filtered using a centrifugal separation filter such that a pH of a filtered liquid was 9.0 or less, and the obtained composite metal hydroxide powder was dried at 120 °C for 24 h or more to generate a composite metal hydroxide. After that, it was heated at 300 °C for 12 h and mixed with the lithium salt at a stoichiometric ratio of 1:1.1. The mixture was calcined at 950 °C for 24 h and recalcined at 500 °C for 24 h in order to obtain the resulting $LiNi_{0.5}Co_{0.2}Mn_{0.3}O_2$ material. The slurry for cathode was prepared by mixing of 84% $LiNi_{0.5}Co_{0.2}Mn_{0.3}O_2$, 8% carbon black (Chevron) as conductor material, 8% polyvinylidene fluoride (Kureha) binder with N-methylpyrrolidinone solvent. The cathode film was formed on the Al foil current collector by slurry coating technique. The coin cell (2032 type) was made of a Li foil for anode, a separator (Celgard), and as-prepared cathode with a 1.3 M $LiPF_6$ electrolyte in a 3:7 ethylene carbonate/diethyl carbonate solvent. The charge/discharge performance was conducted at constant rate of C/10 between 2.7 and 4.3 V on battery test station (WBCS3000, WonATech). High resolution synchrotron X-ray powder diffraction (HRPD) measurements of the samples were carried out at 9B beamline of the Pohang Light Source-II (PLS-II). Pristine $LiNi_{0.5}Co_{0.2}Mn_{0.3}O_2$ powder was scanned from 10° to 130.5° (2θ) at a scan rate of 0.1° min^{-1}. The incident X-rays were vertically collimated using a mirror and monochromatized to a wavelength of 1.54750 Å using a double-crystal Si (1 1 1) monochromator. The detector comprises a set of seven analyzer crystals and seven scintillation detectors with each set separated by 20°. For the thermal stability test of the charged cathode material, the cell was charged at a C/10 rate to a level corresponding to a cathode composition of $Li_{0.33}Ni_{0.5}Co_{0.2}Mn_{0.3}O_2$ and then moved to the glove box for disassembly. The lithium extraction concentrations (x in $Li_{1-x}Ni_{0.5}Co_{0.2}Mn_{0.3}O_2$) were calculated from the elapsed time, current, and mass of the active material in the cathode on the assumption that all current passed was due to lithium insertion. Charged cathode material was peeled off from the current collector and loaded into quartz capillaries in the glove box. Prior sample was cleaned by diethyl carbonate to make an electrolyte-free sample. For the electrolyte containing sample, an excess electrolyte was pipetted in the capillary after unwashed sample was loaded. The capillary was sealed in a glove box before being mounted on the thermal stage of diffract-photometer of beam line X7B, at National Synchrotron Light Source at Brookhaven National Lab. The thermal stage for thermal stability test was heated from 25 to 600 °C with rate of 2.5 °C min^{-1}. The wavelength used at X7B was ~0.3184 Å. The XRD patterns were recorded as a set of circles on a Mar 345-image plate detector in the transmission mode for ~1 min of exposure time. The total recording time for a spectrum was ~2.6 min because of the scanning time of the image plate and transferring time of the spectral information. In order to make an easy comparison with the results in the literature, all the 2θ angles in this paper have been converted to the values corresponding to the wavelength of conventional X-ray tube source with Cu Kα radiation (λ = 1.54 Å).

3. Results and discussion

Fig. 1 shows the high resolution powder diffraction (HRPD) pattern for the $LiNi_{0.5}Co_{0.2}Mn_{0.3}O_2$ powders. All diffraction peaks can be indexed by assuming the structure to be a hexagonal of the α-$NaFeO_2$ type. The HRPD pattern for $LiNi_{0.5}Co_{0.2}Mn_{0.3}O_2$ shows the good separations of the (006)/(012) and the (108)/(110) couples of diffraction lines, which indicates that this pristine $LiNi_{0.5}Co_{0.2}Mn_{0.3}O_2$ material consists of a well-developed layered structure. The oxygen octahedra of the transition metals are edge-shared each other within the octahedral layer and the Li atoms are placed in the lattice channel between interlayer planes. The HRPD pattern does not show any impurity peak and superlattice peaks for Li_2MO_3-like structure representing this material is a single phase layered structure.

Fig. 2 shows the voltage vs. specific capacity profiles of $Li/LiNi_{0.5}Co_{0.2}Mn_{0.3}O_2$ cell between 4.3 V and 2.7 V at a constant rate

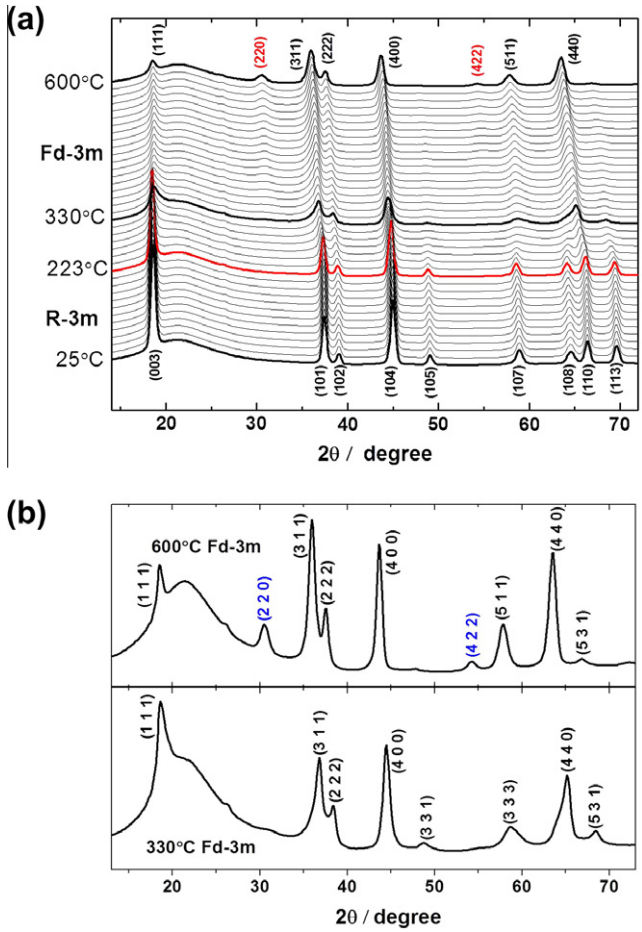

Fig. 3. (a) TR-XRD patterns of the charged $LiNi_{0.5}Co_{0.2}Mn_{0.3}O_2$ in the absence of electrolyte heated from 20 to 600 °C. (b) Two selected XRD patterns from (a) for the sample heated to 330 and 600 °C.

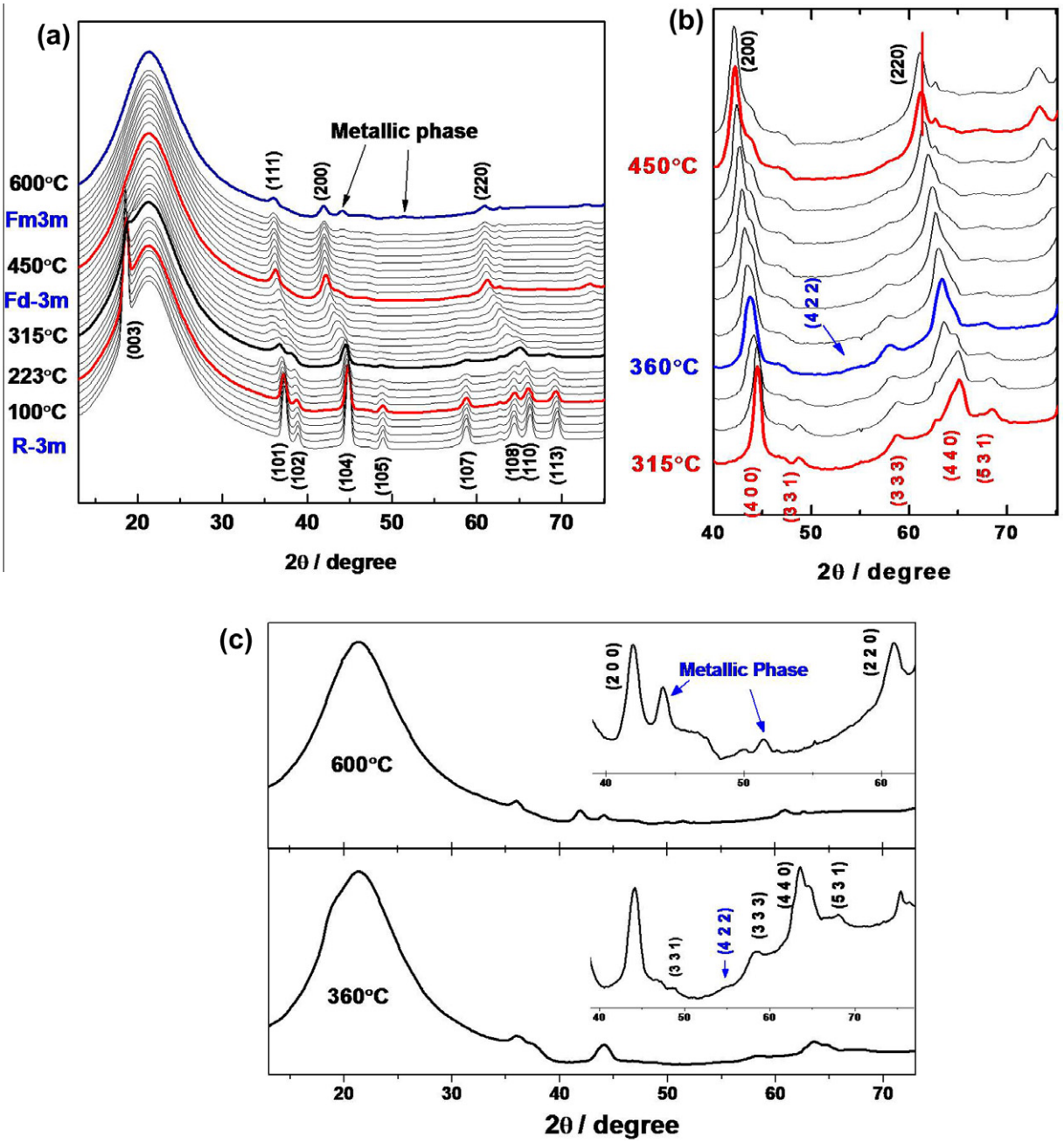

Fig. 4. (a) TR-XRD patterns of the charged $LiNi_{0.5}Co_{0.2}Mn_{0.3}O_2$ in the presence of electrolyte heated from 20 to 600 °C. (b) Magnified XRD patterns from 315 to 475 °C. (c) Two selected XRD patterns from (a) for the sample heated to 360 and 600 °C.

of C/10 for 5 cycles. The theoretical specific capacity of $LiNi_{0.5}Co_{0.2}Mn_{0.3}O_2$ was 277.56 mA h g^{-1}. The first and second charge capacities were 177.3 and 156.6 mA h g^{-1}, respectively and initial irreversible capacity loss of $LiNi_{0.5}Co_{0.2}Mn_{0.3}O_2$ was 21.4 mA h g^{-1}. The cell showed the first discharge capacity of 155.9 mA h g^{-1} and the discharge capacity of 155.7 mA h g^{-1} for second cycle was retained until the fifth cycle. After first cycle, charge/discharge curves were not changed almost to fifth cycle. This indicates that $LiNi_{0.5}Co_{0.2}Mn_{0.3}O_2$ have low irreversible capacity loss and good cyclability compared with other layered structure materials.

The different phase transition behavior of the charged $Li_{0.33}Ni_{0.5}Co_{0.2}Mn_{0.3}O_2$ cathode material with and without electrolyte during thermal stability test was determined using synchrotron based in situ XRD as seen in Figs. 3 and 4. Fig. 3a shows the in situ XRD patterns of $Li_{0.33}Ni_{0.5}Co_{0.2}Mn_{0.3}O_2$ without electrolyte as a function of temperature. The sample at 25 °C showed hexagonal layered structure with a R-3 m space group [23]. The peaks of (108) and (110) in typical layered structure in the temperature range from 223 to 330 °C were emerged to (440) new peak, which was indexed as reflection for the disordered spinel-type structure with a space group of Fd-3m and the disordered spinel-type cubic symmetry was preserved up to 600 °C [24,25]. This indicates that the layered structure in $Li_{0.33}Ni_{0.5}Co_{0.2}Mn_{0.3}O_2$ was transited to a disordered LiM_2O_4-type spinel phase because of increased cation mixing in the temperature range from 223 to 330 °C. In addition, the onset temperature in structural change of $Li_{0.33}Ni_{0.5}Co_{0.2}Mn_{0.3}O_2$ was 223 °C, which was higher than that of $Li_{0.33}NiO_2$ (170 °C) and $Li_{0.27}Ni_{0.8}Co_{0.15}Al_{0.05}O_2$ (200 °C) [26,27]. This means that $LiNi_{0.5}Co_{0.2}Mn_{0.3}$ has better thermal stability than prior Ni based layered structure materials. In the temperature range from 330

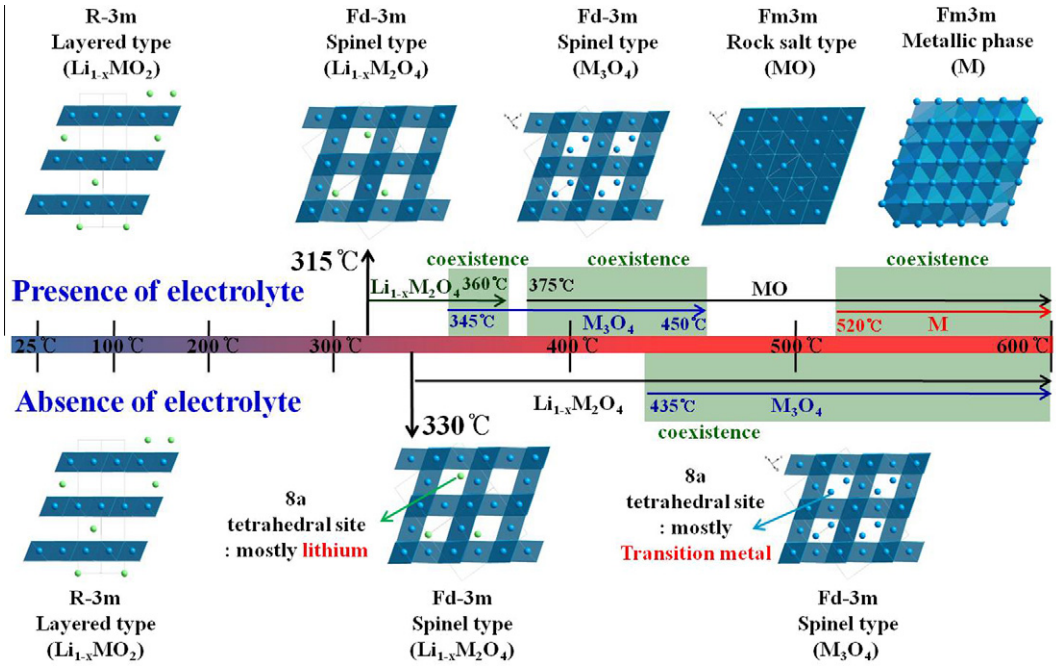

Fig. 5. Schematic illustration of crystal structural changes of the charged $LiNi_{0.5}Co_{0.2}Mn_{0.3}O_2$ in the absence and presence of electrolyte heated from 25 to 600 °C.

to 600 °C, there were noticeable changes in the diffraction lines. The (422) peak which represents the M_3O_4-type spinel structure with the same Fd-3m space group was observed in the temperature range from 330 to 600 °C [28]. In the mean time, the intensity of (331) and (531) peaks was decreased whereas the intensity of (220) line was increased together with new (422) diffraction line with increasing temperature toward 600 °C. This manifests that the disordered LiM_2O_4-type and M_3O_4-type spinel phase were co-existed between 330 °C and 600 °C. This phenomenon can be clearly represented at Fig. 3b. The peaks of (220) and (422) of M_3O_4-type spinel phase were hardly seen in the XRD pattern at 330 °C while the new (220) and (422) peaks of M_3O_4-type spinel phase with the old (331) and (531) peaks of disordered LiM_2O_4-type spinel phase were appeared in the XRD patterns at 600 °C. In addition, the less intensity of the (331) and (531) peaks at 600 °C was observed compared to the ones at 330 °C. The major differences of these two types of spinel phase are the different lattice parameters and different cation distribution [29]. It should be noted that the coexistence of two different types of spinel phase during thermal decomposition has not been observed in other high nickel layered cathodes such as $Li_{1-x}NiO_2$ [27], $Li_{1-x}Ni_{0.89}Al_{0.16}O_2$ [25] and $Li_{1-x}Ni_{0.8}Co_{0.15}Al_{0.05}O_2$ [26]. This might be unique phase transition behavior of Mn containing layered materials only. No further decomposition to MO-type rock salt phase is presented at all up to 600 °C for this sample without electrolyte.

Fig. 4 shows the in situ XRD patterns of $Li_{0.33}Ni_{0.5}Co_{0.2}Mn_{0.3}O_2$ with electrolyte as a function of temperature. Dramatic electrolyte induced structural changes are observed compared to the sample without electrolyte. The $LiMO_2$ layered structure with R-3 m space group was transited to the disordered LiM_2O_4 type spinel structure at temperature range from 223 to 315 °C as seen in Fig. 4a. The ending temperature for the transition from $LiMO_2$ type layered to disordered LiM_2O_4 type phase in the presence of electrolyte was 315 °C, which was higher than that of $Li_{0.27}Ni_{0.8}Co_{0.15}Al_{0.05}O_2$ (280 °C) and $Li_{0.33}Ni_{1/3}Co_{1/3}Mn_{1/3}O_2$ (304 °C) [26–28].

The intensity of (331) and (531) peaks got weaker while the temperature increased from 315 to 360 °C as seen in Fig. 4b. The (422) peak was observed in the temperature range from 345 to 360 °C. In the temperature range from 345 to 360 °C, the disordered LiM_2O_4-type and M_3O_4-type spinel phase were co-existed. As seen in Fig. 4c, we can observe the peaks of (331), (531), (422) and (440) in the XRD patterns at 360 °C. The new two peaks which were confirmed as reflactions of MO-type rock salt phase at the left side of the disordered M_3O_4-type spinel phase appeared from 375 to 600 °C. This demonstrates that the disordered M_3O_4-type spinel structure was transited to MO-type rock salt phase and co-existed with MO-type rock salt phase with increasing temperature from 375 to 450 °C. In addition, the onset temperature of MO-type rock salt phase in $Li_{0.33}Ni_{0.5}Co_{0.2}Mn_{0.3}O_2$ was 375 °C, which was much higher than that of $Li_{0.27}Ni_{0.8}Co_{0.15}Al_{0.05}O_2$ (290 °C) and slightly lower than that of $Li_{0.33}Ni_{1/3}Co_{1/3}Mn_{1/3}O_2$ (400 °C) [25,26,28]. The phase transitions from the spinel-type phase to the rock salt-type phase produce substantial amount of heat accompanied by releasing oxygen since the thermal decomposition to the rock salt structure is a exothermic reaction [30,31]. The better thermal stability of the $LiNi_{0.5}Co_{0.2}Mn_{0.3}O_2$ than other high nickel layered materials like $LiNi_{0.8}Co_{0.15}Al_{0.05}O_2$ can be attributed to the higher onset temperature of thermal decomposition to the rock salt phase during heating. As seen in Fig. 4a, metallic Ni phase was observed from 520 °C. In the end of the test temperature (600 °C), metallic Ni phase and MO-type rock salt phase were co-existed as shown in Fig. 4c. The electrolyte accelerates the degradation of the cathode material by promoting decomposition reaction of active materials in cathode [32].

Fig. 5 shows schematic illustration of crystal structure changes in the charged $Li_{0.33}Ni_{0.5}Co_{0.2}Mn_{0.3}O_2$ with and without electrolyte as a function of temperature. The charged $Li_{0.33}Ni_{0.5}Co_{0.2}Mn_{0.3}O_2$ without electrolyte shows higher beginning and ending temperature of the phase transition from layered to the spinel-type phases than the one with electrolyte indicating the dramatic effect of the presence of electrolyte on the thermal stability of the charged cathode materials. Compared to the previous nickel based layered materials, the structural stability of the $LiNi_{0.5}Co_{0.2}Mn_{0.3}O_2$ during heating is better than that of other high nickel layered materials and comparable to that of low nickel $LiNi_{1-y-z}Mn_yCo_zO_2$ [28].

4. Conclusions

In situ XRD analysis has been carried out to investigate the thermal decomposition reaction of charged $Li_{0.33}Ni_{0.5}Co_{0.2}Mn_{0.3}O_2$ cathode materials with and without electrolyte during heating from 25 to 600 °C. The in situ XRD results for charged $Li_{0.33}Ni_{0.5}Co_{0.2}Mn_{0.3}O_2$ cathode materials without electrolyte show that the original layered structure converts to a disordered LiM_2O_4-type spinel structure first, then the formation of another M_3O_4-type spinel structure co-existing with the disordered spinel phase. The electrolyte induced structural changes are clearly observed in the in situ XRD results for charged $Li_{0.33}Ni_{0.5}Co_{0.2}Mn_{0.3}O_2$ cathode materials with electrolyte compared to the one without electrolyte. The charged $Li_{0.33}Ni_{0.5}Co_{0.2}Mn_{0.3}O_2$ cathode materials with electrolyte show lower onset temperature of phase transition from layered phase to spinel phases and the further decomposition to MO-type rock salt phase even with the formation of metallic phase at the end of heating. Compared to the previous nickel based layered materials, the structural stability of the $LiNi_{0.5}Co_{0.2}Mn_{0.3}O_2$ during heating is better than that of other high nickel layered materials and comparable to that of low nickel $Li_{0.33}Ni_{1/3}Co_{1/3}Mn_{1/3}O_2$.

Acknowledgements

This work was supported by the IT R&D program (KI0018-10039182, 10041856) of the KEIT funded by the Ministry of Knowledge Economy. This work was also supported by the Fundamental R&D Program for Technology of World Premier Materials and Energy Efficiency & Resources (2010T100200295) of Ministry of Knowledge Economy. The work done at Brookhaven National Lab. was supported by the U.S. Department of Energy, the Assistant Secretary for Energy Efficiency and Renewable Energy, Office of Vehicle Technologies under Contract Number DEAC02-98CH10886. This work was partly supported by the National Research Foundation funded by the Korean Government (MEST: NRF-2010-0029065 & R31-2008-10029).

References

[1] J.R. Dahn, E.W. Fuller, M. Obrovac, U. Von Sacken, Solid State Ionics 69 (1994) 265–270.
[2] D. Du Pasquier, F. Disma, T. Bowmer, A.S. Gozdz, G. Amatucci, J.M. Tarascon, J. Electrochem. Soc. 145 (1998) 472–477.
[3] S.I. Tobishima, K. Takei, Y. Sakurai, J.I. Yamaki, J. Power Sources 90 (2000) 188–195.
[4] Z. Lu, D.D. MacNeil, J.R. Dahn, Electrochem. Solid-State Lett. 4 (2002) A200–A203.
[5] N. Yabuuch, T. Ohzuku, J. Power Sources 119–121 (2003) 171–174.
[6] I. Belharouak, Y.K. Sun, J. Lui, K. Amine, J. Power Sources 123 (2003) 247–252.
[7] S. Zhang, C. Deng, S.Y. Yang, H. Niu, J. Alloys Comp. 484 (2009) 519–523.
[8] C. Deng, S. Zhang, B.L. Fu, S.Y. Yang, L. Ma, J. Alloys Comp. 496 (2010) 521–527.
[9] C.-H. Lu, B.-J. Shen, J. Alloys Comp. 497 (2010) 159–165.
[10] C. Delmas, I. Saadoune, A. Rougier, J. Power Sources 43 (1993) 595–602.
[11] C.S. Johnson, J.-S. Kim, A.J. Kropf, A.J. Kahaian, J.T. Vaughey, L.M. Fransson, K. Edstrom, M.M. Thackeray, Chem. Mater. 15 (2003) 2313–2322.
[12] J.K. Ngala, N.A. Chernova, M. Ma, M. Mamak, P.Y. Zavalij, M.S. Whittingham, J. Mater. Chem. 14 (2004) 214–219.
[13] M.S. Whittingham, Chem. Rev. 104 (2004) 4271–4301.
[14] D. Zeng, J. Cabana, J. Breger, W.-S. Yoon, C.P. Grey, Chem. Mater. 19 (2007) 6277–6289.
[15] K. Ben-Kamel, N. Amdouni, A. Mauger, C.M. Julien, J. Alloys Comp. 528 (2012) 91–98.
[16] D. Li, Y. Sasaki, M. Kageyama, K. Kobayakawa, Y. Sato, J. Power Sources 148 (2005) 85–89.
[17] S. Lee, D. Jang, J. Yoon, Y.-H. Cho, Y.-S. Lee, D.-H. Kim, W.-S. Kim, W.-S. Yoon, J. Electrochem. Sci. Technol. 3 (2012) 29–34.
[18] S.-B. Kim, K.J. Lee, W.J. Choi, W.-S. Kim, I.C. Jang, H.H. Lim, Y.S. Lee, J. Solid State Electrochem. 14 (2012) 919–922.
[19] W. Liu, M. Wang, X.I. Gao, W. Zhang, J. Chen, H. Zhou, Z. Zhang, J. Alloys Comp. 543 (2012) 181–188.
[20] J.-Z. Kong, F. Zhou, C.-B. Wang, Z.-Y. Yang, H.-F. Zhai, H. Li, J.-X. Li, Z. Tang, S.-Q. Zhang, J. Alloys Comp. 554 (2013) 221–226.
[21] W.-S. Kim, S.-B. Kim, Y.J. Heo, S.T. Koh (2008) IMLB 2008 (277).
[22] M.H. Lee, Y.J. Kang, S.T. Myung, Y.K. Sun, Electrochem. Acta 50 (2004) 939–948.
[23] T. Ohzuku, A. Ueda, J. Electrochem. Soc. 141 (1994) 2972–2977.
[24] J.N. Reimers, W. Li, J.R. Dahn, Phy. Rev. B47 (1993) 8486–8493.
[25] M. Guilmard, L. Croquennec, D. Denux, C. Delmas, Chem. Mater. 15 (2003) 4476–4483.
[26] W.-S. Yoon, M. Balasubramanian, X.Q. Yang, J. McBreen, J. Hanson, Electrochem Solid-State Lett. 8 (2005) A83–A86.
[27] W.-S. Yoon, J. Hanson, J. Mcbreen, X.Q. Yang, Electrochem. Commun. 8 (2006) 859–862.
[28] K.-W. Nam, W.-S. Yoon, X.Q. Yang, J. Power Sources 189 (2009) 515–518.
[29] N. Yabuuchi, Y-T Kim, H.H. Li, Y. Shao-Horn, Chem. Mater. 20 (2008) 4936–4951.
[30] H. Arai, S. Okada, Y. Sakurai, J. Yamaki, Solid State Ionics 109 (1998) 295–302.
[31] K.-K. Lee, W.-S. Yoon, K.-B. Kim, J. Electrochem. Soc. 148 (2001) A1164–A1170.
[32] L. Wang, T. Maxish, G. Ceder, Chem. Mater. 19 (2007) 543–552.